

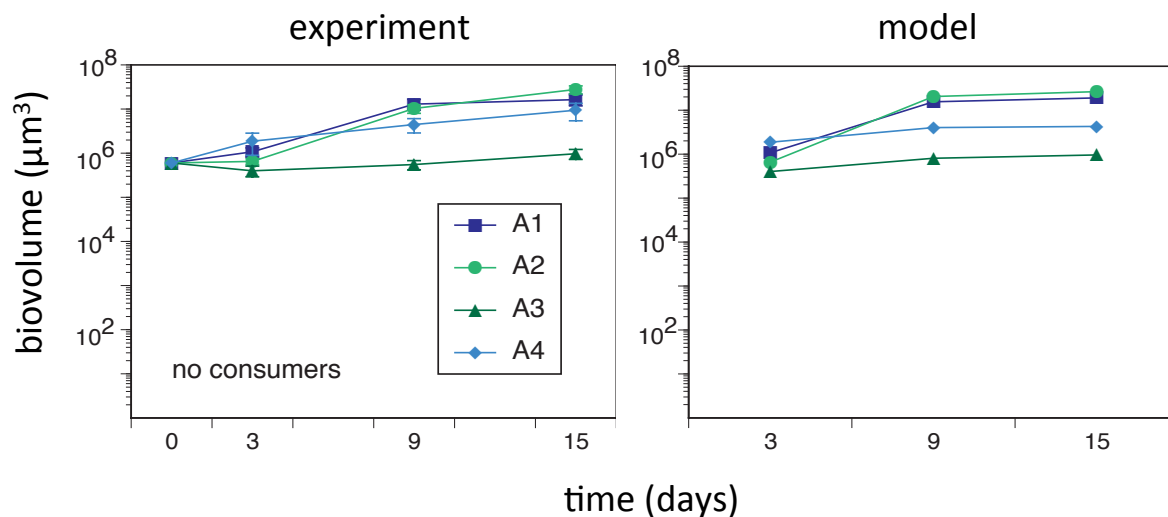
Filip, J., Bauer, B., Hillebrand, H., Beniermann, A., Gaedke, U. and Moorthi, S. D. 2014. Multitrophic diversity effects depend on consumer specialization and species-specific growth and grazing rates. – Oikos doi: 10.1111/oik.01219

## Appendix 1

### Model parametrization

We determined algal maximum growth rates ( $r_i'$ ) by fitting the model to the observed time series of the mean algal biovolume in the diversity experiment in the treatment without consumers (Fig. A1.1). We used the mean of day 3 as the starting biovolume for the simulations.

Figure A1.1. Temporal development of algal biovolume in the experiment (left: mean  $\pm$  SE) and simulated values (right). Note that the model simulation starts on day 3 instead of day 0, as the process of ciliate mortality due to the experimental inoculation procedure is not considered in the model. Please also note that the simulated slope of increase in the exponential growth phase (ca between days 3–9), which is the graphical representation of the maximum growth rate, matches the empirical data well. Standard deviations of biovolumes at the last sampling day were: A1 =  $9.1 \times 10^6$ , A2 =  $1.1 \times 10^7$ , A3 =  $4.9 \times 10^5$ , A4 =  $8.1 \times 10^6$   $\mu\text{m}^3 \text{ml}^{-1}$ , that is, the absolute values of biovolume estimated by the model are well within the range observed in the experiment.

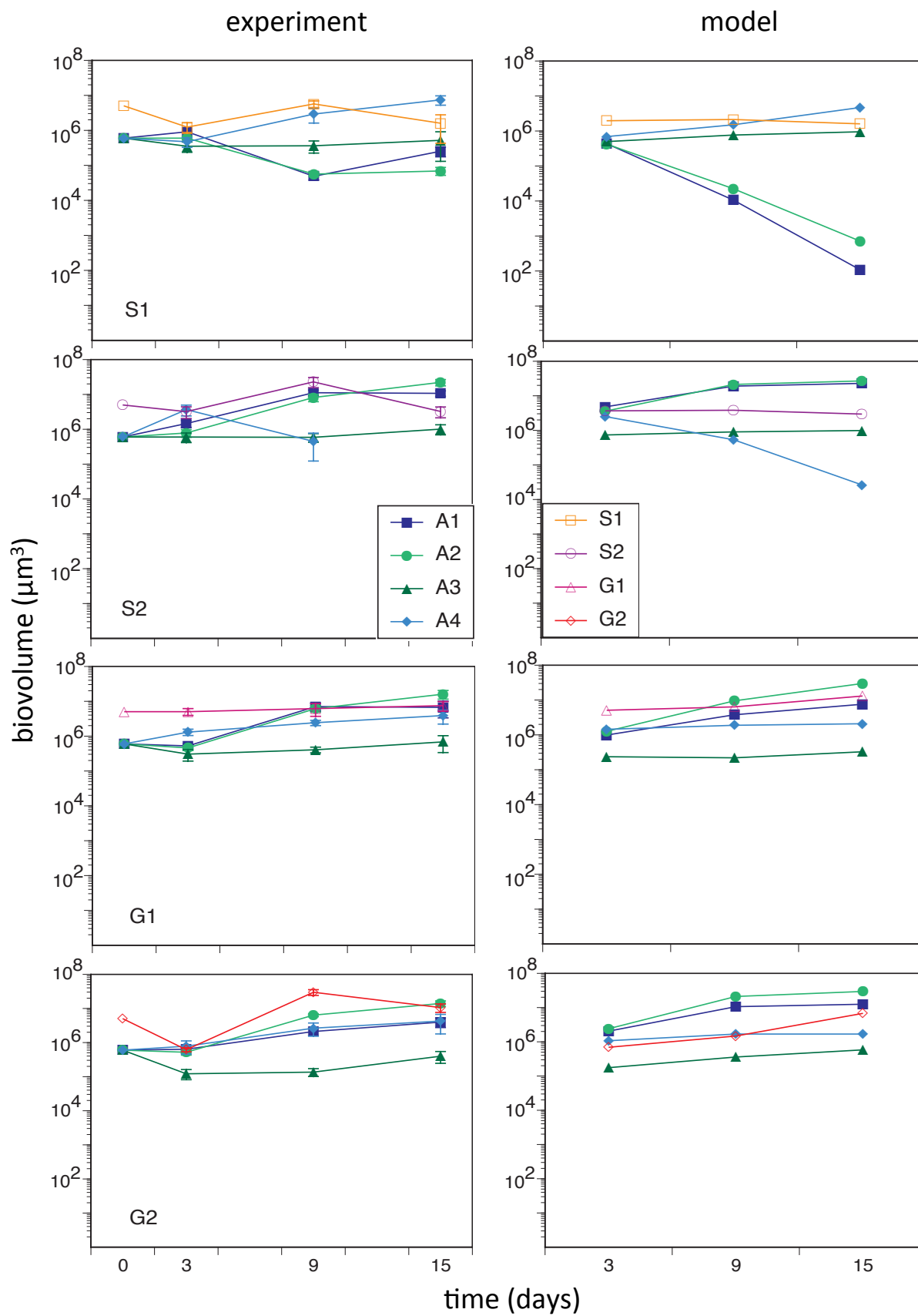


The summed biovolume of A1, A2 and A4 was  $5.4 \times 10^7 \pm 2.1 \times 10^7 \mu\text{m}^3 \text{ml}^{-1}$  at the end of the experiment in the treatment without consumers. The corresponding value for A3 was  $9.7 \times 10^5 \pm 4.3 \times 10^5 \mu\text{m}^3 \text{ml}^{-1}$ . The common carrying capacity of A1, A2 and A4 ( $5 \times 10^7 \mu\text{m}^3 \text{ml}^{-1}$ ) and that of A3 ( $10^6 \mu\text{m}^3 \text{ml}^{-1}$ ) used in the model are well within this range. A separate carrying capacity for A3 was included as it was mostly limited by silica for which it was not competing with other algae.

Grazing rates and feeding preferences of the consumers were determined based on the monoculture treatments of the diversity experiment, where each consumer was separately fed with a mixture of the four algae (Fig. A1.2). The only exception was S2, which behaved idiosyncratically among the different treatments and its grazing rate was set, somewhat arbitrarily, to a relatively low value. However, the grazing rate of S2 did not play a substantial role in the model outcome. A higher grazing rate of this species did not change the prey biovolume or evenness greatly in the treatments without S1, where the prey of S2, A4, was anyway limited by competition with A1 and A2. In the treatments with S1, a higher grazing rate of S2 only increased the overall prey biovolume reduction by reducing the biovolume of A4, i.e. somewhat strengthened the biovolume decreasing effect of S1.

We obtained a value of  $6.5 \times 10^6 \mu\text{m}^3 \text{ml}^{-1}$  for the half-saturation constant by fitting. This value corresponds to  $1.3 \text{ mg C l}^{-1}$ , using a conversion factor of  $0.2 \text{ pg C } \mu\text{m}^{-3}$  (Menden-Deuer and Lessard 2000). The values of  $0.05 \text{ d}^{-1}$  and  $0.35$  for the mortality rate and growth efficiency for the predators are in line with values used elsewhere (Tirok and Gaedke 2010, Aberle et al. 2012). Although it is likely that different algal species had different palatabilities for the different consumers, we did not have sufficiently accurate data for quantifying these differences. Thus, to keep the number of free parameters at a minimum, we used the same growth efficiency for all consumers regardless of the prey identity.

Figure A1.2. Temporal development of algal and ciliate biovolume in the experiment (left column; mean +/- standard error) and simulated values (right column). The temporal changes in the biovolume are mostly well described by the model. Note that the model simulation starts on day 3 instead of day 0, as the process of ciliate mortality due to the experimental inoculation procedure is not considered in the model.



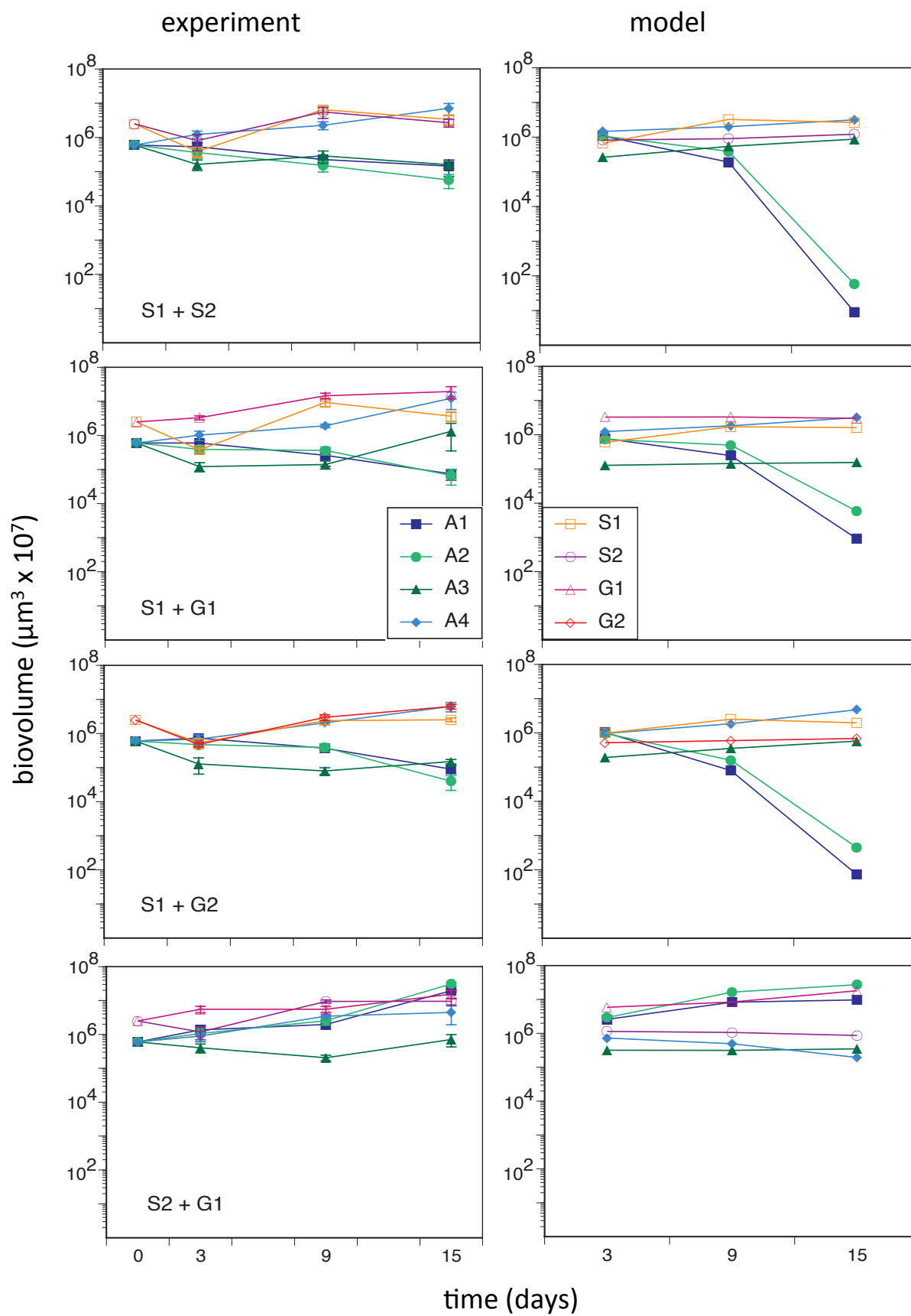
## Appendix 2

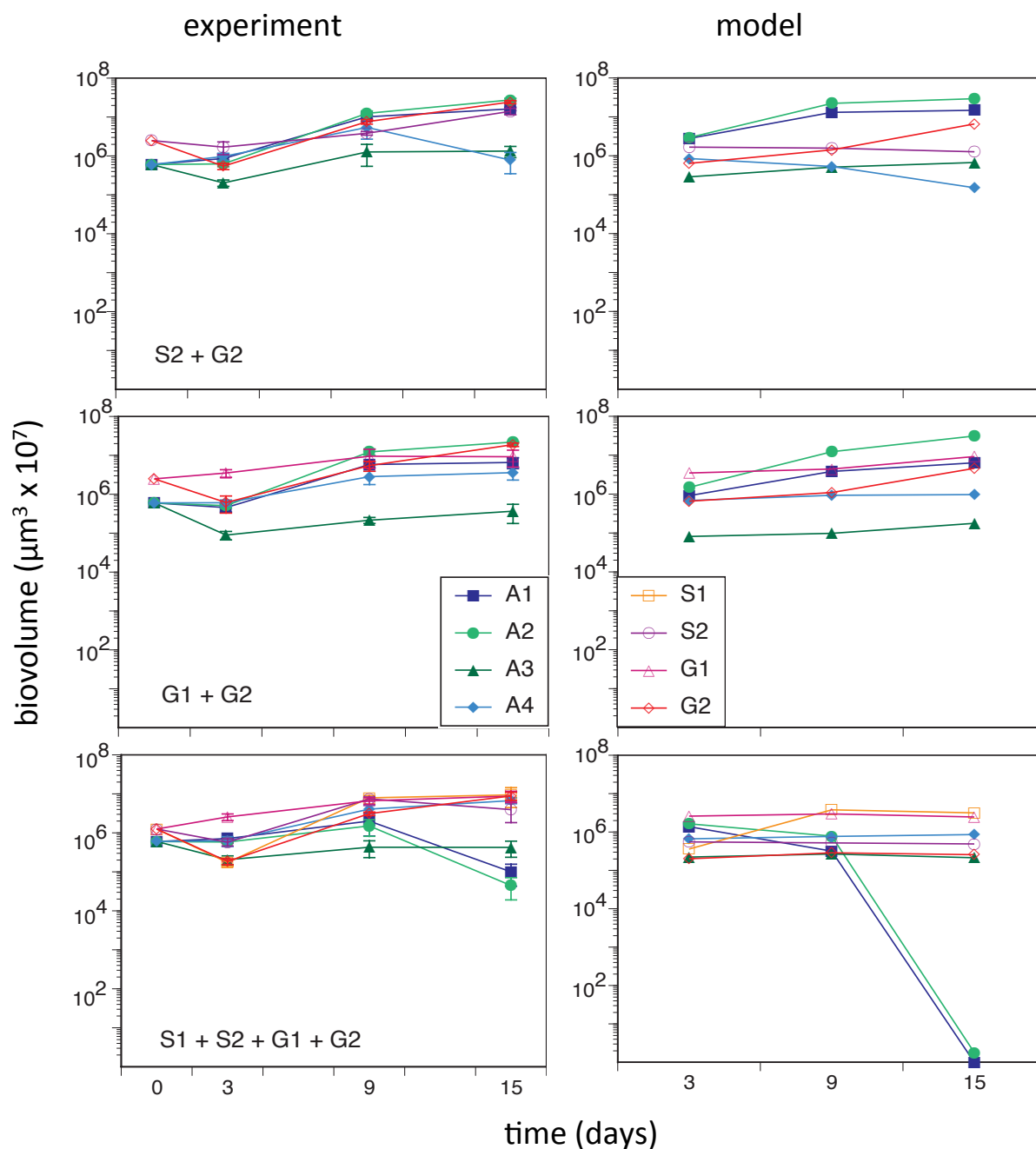
### Temporal development of ciliate and prey biovolume as well as ciliate abundances in the multispecies consumer treatments

In the multispecies consumer treatments we observed dampened biovolume dynamics (Fig. A2.1) compared to monoculture consumer treatments (Supplementary material Appendix 1 Fig. A1.2). In general, consumer biovolume decreased from day 0 to day 3 (mortality due to pipetting and inoculation procedure during experimental setup), then increased from day 3 to 9 and stayed constant afterwards. One exception was S1 in combination with S2 and G1 since S1 decreased after day 9.

The model generally predicted somewhat less fluctuating biomasses than observed (both in the one consumer and multispecies consumer treatments, see also A1.2 in Supplementary material Appendix 1), but the direction of biovolume change matched the experimental data well. Consumer biovolume first increased, then stayed constant except for S1, where mostly a slight decrease from day 9 to day 15 was predicted. For S1, the model suggested that the decrease of its biomass was due to an overexploitation of its prey, as A1 and A2 strongly decreased in the presence of S1. This decrease in A1 and A2 was also observed in the experiment, although it was less pronounced than in the model. In the absence of S1, both in the experiment and the model, A1 and A2 showed increasing to constant biovolume, as these algae were not consumed at such high rates, while the less productive algae A3 and A4 reached lower biovolume. This suggested that the algae and their consumers approached an equilibrium during the experiment.

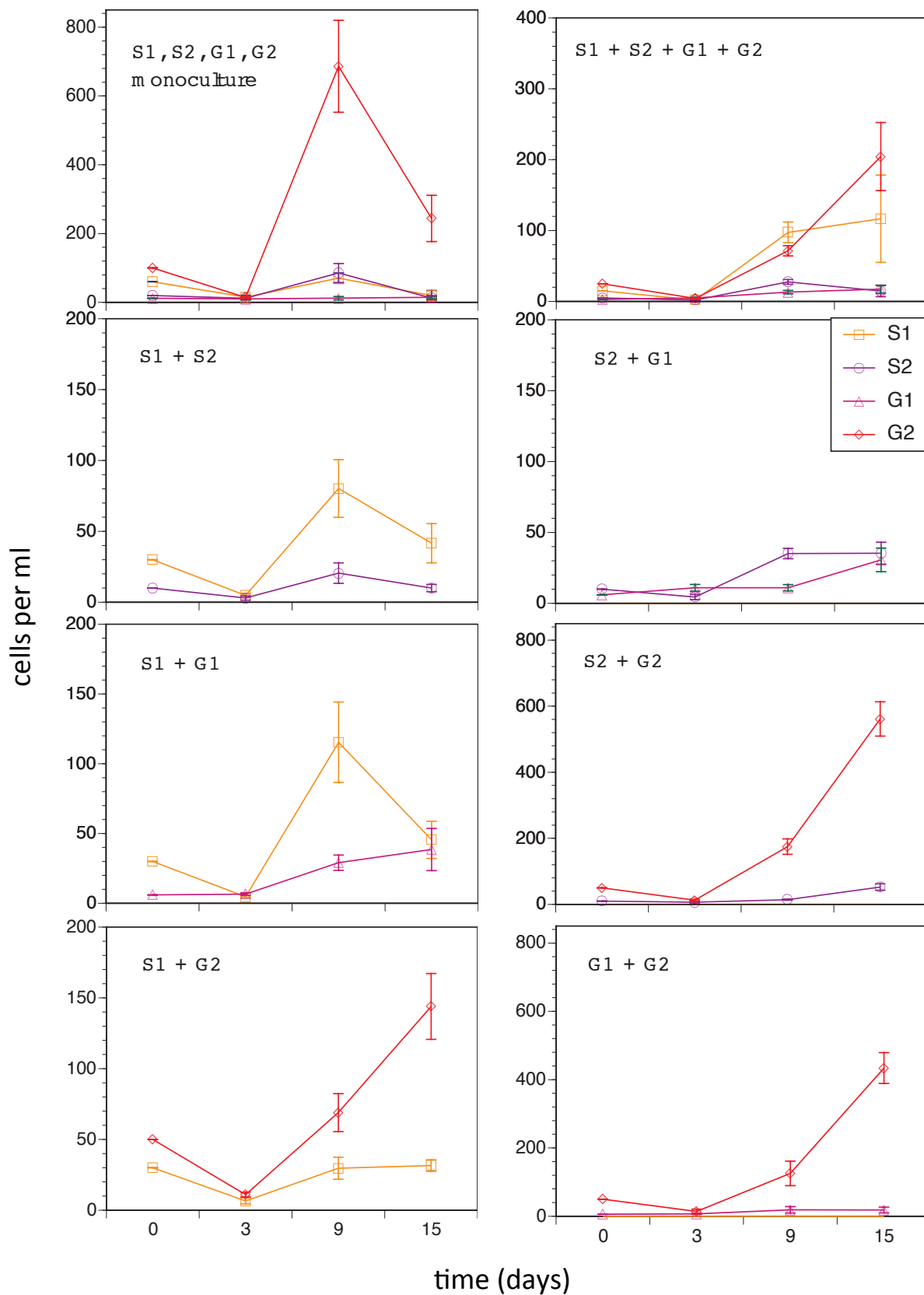
Figure A2.1. Temporal development of algal and ciliate biovolume in the experiment (left column; mean  $\pm$  standard error) and simulated values (right column). Note that the model simulation starts on day 3 instead of day 0, as the process of ciliate mortality due to the experimental inoculation procedure is not considered in the model.





Individual ciliate cell volumes amounted to  $8 \times 10^4 \mu\text{m}^3$  for S1,  $2.7 \times 10^5 \mu\text{m}^3$  for S2,  $5 \times 10^5 \mu\text{m}^3$  for G1 and  $4.3 \times 10^4 \mu\text{m}^3$  for G2 and were assumed to be constant during the experiment. Hence, the temporal development of species-specific cell abundances shows the same pattern as their biovolume (A2.1, A2.2). The smallest ciliate G2 reached highest abundances in monoculture and in all multispecies consumer combinations (A2.2).

Figure A2.2. Temporal development of ciliate cell abundances from the start of the experiment (day 0) until the end (day 15). Values represent the mean of four replicates + standard error. Note the different scaling on the y-axes.



## References

- Aberle, N. et al. Warming induces shifts in microzooplankton phenology and reduces time-lags between phytoplankton and protozoan production. – *Mar. Biol.* 159: 2441–2453.
- Menden-Deuer, S. and Lessard E. J. 2000. Carbon to volume relationships for dinoflagellates, diatoms, and other protist plankton. – *Limnol. Oceanogr.* 45: 569–579.
- Tirok, K. and Gaedke U. 2010. Internally driven alternation of functional traits in a multispecies predator–prey system. – *Ecology* 91: 1748–1762.